

# Fabrication and Characterization of Benzocyclobutene Optical Waveguides by UV Pulsed-Laser Illumination

Liang-Yin Chen, *Student Member, IEEE*, Wan-Shao Tsai, *Student Member, IEEE*, Wen-Hao Hsu, Kuan-Yu Chen, and Way-Seen Wang, *Member, IEEE*

**Abstract**—Buried-type benzocyclobutene (BCB) optical waveguides fabricated by UV pulsed-laser illumination are proposed and comprehensively characterized in this paper. The fabrication process is greatly simplified as compared to conventional dry-etched ridge-type BCB waveguides. The measured propagation loss at 1548 nm is as low as 0.6 dB/cm due to the buried waveguide structure. And the produced refractive index change is dependent upon the number of laser shots such that single-mode waveguides with different mode sizes can be tailored for efficient coupling. Furthermore, rigorous analyses of surface damage threshold, rms roughness, and chemical characteristics under different illumination conditions are presented to illustrate the design considerations and the chemical mechanism of the UV-induced BCB waveguides.

**Index Terms**—Benzocyclobutene (BCB), excimer lasers, optical polymers, optical waveguides.

## I. INTRODUCTION

POLYMER-BASED optical waveguides and devices are attractive for integrated optic fields, such as optical communication and optical interconnection due to their versatility in terms of material properties, simple fabrication process, and low cost [1]–[4]. Among various polymer materials, benzocyclobutene (BCB) has been widely used in multilayer interconnection, flat panel display, and microelectronic packaging, etc [5]–[8]. Due to its great material properties, including excellent planarization, low dielectric constant, low moisture absorption, low optical loss, high chemical resistance, and high thermal stability (high glass transition temperature) [9], [10], BCB has also been used for optical waveguides in recent years [11]–[13]. The major conventional fabrication methods for BCB waveguides include etching by reactive ion etching (RIE) and patterning photo-sensitive type BCB [5]. However, the etching method by RIE is more cumbersome and forms waveguides in a ridged structure, which, in general, causes higher loss due to the sidewall roughness, especially at shorter wavelengths [14]. As for the photo-sensitive BCB, a photo initiator must be added

to the resin, and thus the preservation is much more difficult. Recently, several methods for the fabrication of waveguides without RIE process were proposed. In particular, the fabrication of buried-channel waveguides by direct illumination of deep-ultraviolet light through a quartz-chromium mask on polymethyl methacrylate (PMMA) has been reported [15]. The technique requires no further etching and development process and uses only a single polymer layer. For BCB, due to its strong absorption at wavelength shorter than 300 nm [14], we replaced the light source by a krypton fluorine (KrF) excimer laser of wavelength 248 nm [16]. Experimental results showed that buried-type BCB channel waveguides on silicon substrate can be successfully fabricated such that the sidewall roughness can be minimized. Moreover, BCB on silicon substrate is compatible with the standard processing techniques of integrated circuits [17].

In this work, more results of the proposed UV-illumination method for buried-type BCB channel waveguides are reported. The uniform refractive index changes, verified by the inverse Wentzel–Kramers–Brillouin (IWKB) method [18], are varying from  $1 \times 10^{-3}$  to  $4 \times 10^{-3}$  and dependent on the number of laser shots, such that single-mode waveguides with different mode sizes can be tailored for efficient coupling to semiconductor laser diodes [19]. Furthermore, chemical properties of surface damage threshold, root-mean-square (rms) roughness, changes of chemical functional groups, and changes of atom percentages are characterized by scanning electron microscopy (SEM), atomic force microscopy (AFM), Fourier transform infrared (FTIR) spectroscopy, and X-ray photoelectron spectroscopy (XPS) to analyze the chemical mechanism behind the UV-illumination and find the process parameters suitable for the fabrication of the waveguides.

In the next section, the process for the fabrication of buried-type BCB waveguides and the experimental setup for UV illumination are described. Then in Section III, results of UV-induced index changes, surface damage caused by pulsed-laser, and adjustable single-mode optical waveguides are presented. Moreover, chemical characteristics behind the UV-illuminated BCB and the mechanism of UV-illuminated index change are further addressed.

## II. EXPERIMENTAL PROCESS

The procedure for the fabrication of BCB waveguides on a silicon substrate is illustrated in Fig. 1. After cleaning the silicon wafer, a SiO<sub>2</sub> layer of thickness 7.7 μm is grown on the silicon substrate as a lower cladding layer by plasma enhanced chemical vapor deposition. A BCB layer of 1.7 μm is then spin-coated on top of the SiO<sub>2</sub> layer. After soft curing in the oven, the wafer

Manuscript received July 14, 2006; revised November 28, 2006. This work was supported by National Science Council, Taipei, Taiwan, R.O.C., under Contract NSC 95-2221-E-002-326-MY3.

L.-Y. Chen, W.-H. Hsu, and K.-Y. Chen are with the Graduate Institute of Electro-Optical Engineering, National Taiwan University, Taipei, Taiwan 106, R.O.C. (e-mail: f91943031@ntu.edu.tw; hsiusimon@msn.com; b89901020@ntu.edu.tw).

W.-S. Tsai is with the Graduate Institute of Electronics Engineering, National Taiwan University, Taipei, Taiwan 106, R.O.C. (e-mail: f91943030@ntu.edu.tw).

W.-S. Wang is with the Department of Electrical Engineering, National Taiwan University, Taipei, Taiwan 106, R.O.C. (e-mail: wswang@cc.ee.ntu.edu.tw).

Digital Object Identifier 10.1109/JQE.2006.890400

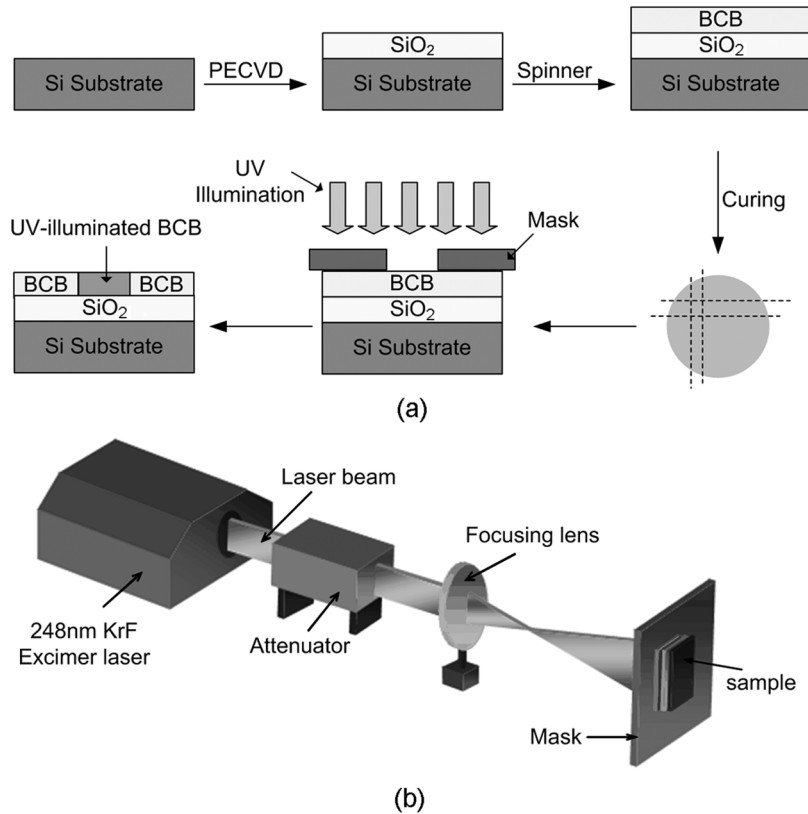


Fig. 1. Fabrication process of the buried-type BCB channel waveguides by UV illumination. (a) Process steps. (b) Experimental setup.

is put in a nitrogen flowing furnace at 250 °C for 1 h. Under this condition, 98%–100% of BCB can be thermally cured [20] and the original liquid BCB monomer is now converted into polymer in a solid-state thin film. Finally, the wafer is cut into suitable sizes for UV illumination and index measurement.

The UV source used is a KrF excimer laser of wavelength 248 nm with a pulsewidth of 10 ns. The energy density of incident UV pulses before being expanded is controlled at 100 mJ/cm<sup>2</sup>, and the repetition rate is set at 5 Hz. A schematic diagram of the UV-illumination setup is shown in Fig. 1(b). An attenuator is used to control the output power. A fused silica focusing lens with a focusing length of 15 cm is used to expand the laser beam size. For the ease of alignment, the sample holder is placed at a distance of three times the focal length behind the focusing lens, so that the laser beam size can be expanded large enough to cover the whole sample without the need of beam scanning. The optical path and sample stage position are then adjusted with a thermal paper to verify the uniformity of the laser beam. For an efficient illumination, contact printing is adopted through a quartz-chromium mask. The laser pulses are then allowed to pass through the mask to change the index of the illuminated BCB areas.

### III. EXPERIMENTAL RESULTS AND DISCUSSION

#### A. UV-Induced Refractive Index Changes

In the refractive index measurement, a prism coupler (Metricon 2010) is used. All samples are measured before UV-illumination to get original indexes as references. Two sets of measured samples are used to verify the repeatability of the

method. For each sample, three independent measurements are made and the averages are found. Based on Metricon 2010 operation guide and several measurements of standard samples, of which the index values are already known, an index accuracy of  $\pm 0.001$  can be verified. Results show that the errors (difference between measured values and averages) are all smaller than 0.0003, which shows good accuracy in our measurement. Fig. 2 shows the averages with error margins of refractive index changes induced by different numbers of laser shots. When less than 100 laser shots are illuminated, the index changes increase rapidly with the number of laser shots and then slow down gradually. When the number of laser shots is greater than 300, index changes tend to be constant. Moreover, the index changes are weakly dependent on wavelength and almost independent of polarization. From our experience, the measured refractive index change  $\Delta n$  can be suitably fitted to an equation as given by

$$\Delta n = \Delta n_{\max} \left\{ \frac{(N/N_c)}{[1 + (N/N_c)^\alpha]^{1/\alpha}} \right\} \quad (1)$$

where  $N$  is the number of laser shots and  $\Delta n_{\max}$ ,  $N_c$ , and  $\alpha$  are fitting parameters as listed in Table I.

In order to verify the index distribution of BCB films, prism measurements followed by the IWKB method implantation are adopted, which is a general method for index profiling of an optical waveguide. For this measurement, another thicker BCB film is prepared, in which waveguides supporting multimodes are required. In the index measurement, a film thickness of 6.7  $\mu\text{m}$  and 11 modal effective indices are obtained

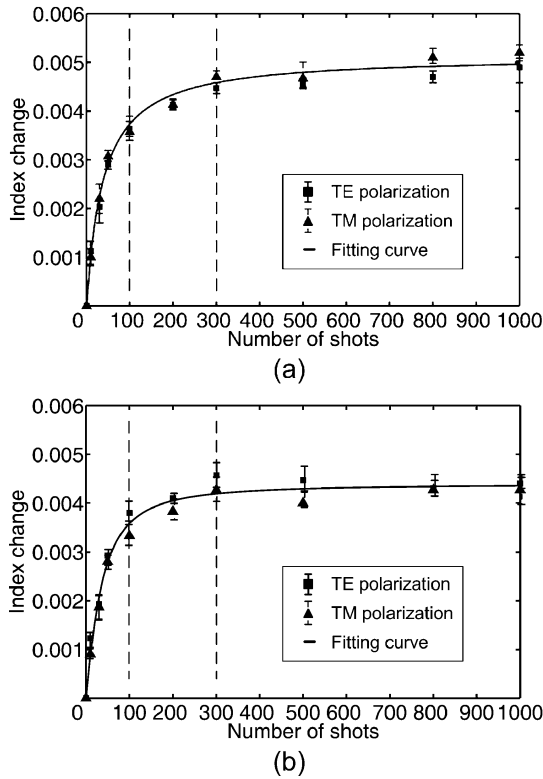


Fig. 2. Measured index changes versus number of laser shots for TE and TM polarization at (a) 632.8 nm and (b) 1548 nm.

TABLE I  
FITTING PARAMETERS

| Wavelength<br>(nm) | Fitting parameters |       |          |
|--------------------|--------------------|-------|----------|
|                    | $\Delta n_{\max}$  | $N_c$ | $\alpha$ |
| 632.8              | 0.0051             | 40    | 1.005    |
| 1548               | 0.0044             | 48    | 1.455    |

by the prism coupler. The adopted IWKB method is given in [18], which is used to retrieve the shape of the index profile from the measured modal effective indices. The approximation is for index profile of decreasing monotonically from the surface. When an index profile of step distribution is performed, the approximation overshoots near the turning point. A test of the step-index distribution of an entire un-illuminated BCB film on a silica layer is done first as shown in Fig. 3(a). Based on the analysis in [18], the overshoots near the turning point represent a step-index distribution and the film thickness agrees with the value measured by the prism coupler. After an illumination of 100 laser shots, the profile is shown in Fig. 3(b), in which the induced index change of entire BCB film is  $4 \times 10^{-3}$  and reveals a step-profile distribution. The verified step-index profile caused by UV-illumination indicates that the UV illumination on BCB is promising for making deep grating on the film.

**B. Surface Damage and Propagation Loss of BCB Film**

As laser beam traces appear on BCB films when over 500 laser shots are illuminated, laser-caused surface damage on illuminated samples is of interest to be investigated by SEM and

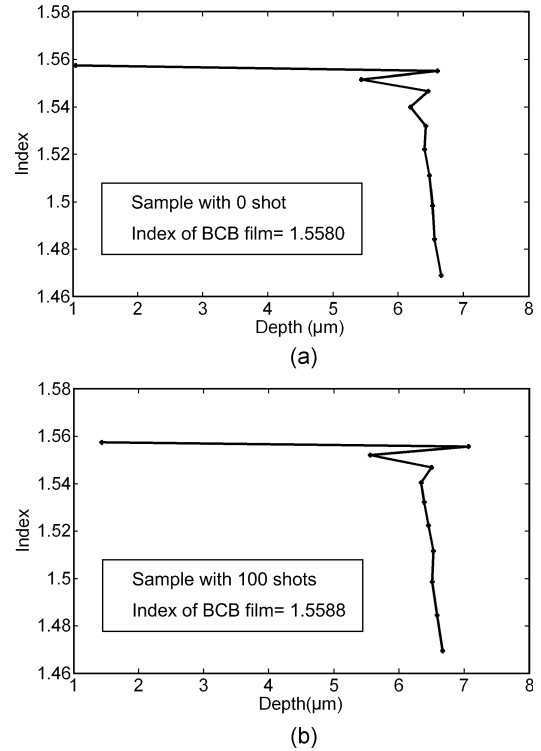


Fig. 3. Index profiles of 6.7- $\mu\text{m}$  BCB films illuminated by (a) 0 shot and (b) 100 shots.

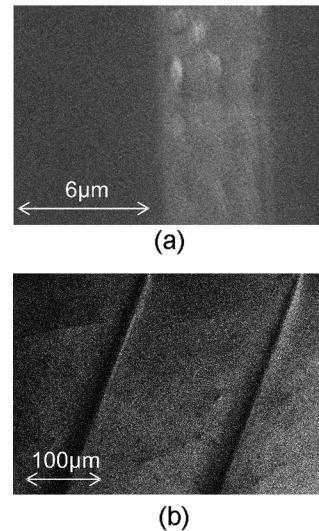


Fig. 4. SEM photos of BCB films illuminated by (a) 200 shots and (b) 1000 shots.

AFM. Results show that the surfaces of BCB films with less than 100 laser shots are almost the same as that without any laser shot. As a BCB film is illuminated with more than 100 laser shots, surface damage emerges due to the accumulation of high energy within a short time on the polymer material. Fig. 4(a) is the photo at higher magnification, and we can see that the patterns of waveguides are slightly puffed up after 200 laser shots are illuminated. For more numbers of laser shots, e.g., 1000 laser shots, damages are clearer such that the raised structure can be easily observed at lower magnification shown in Fig. 4(b).

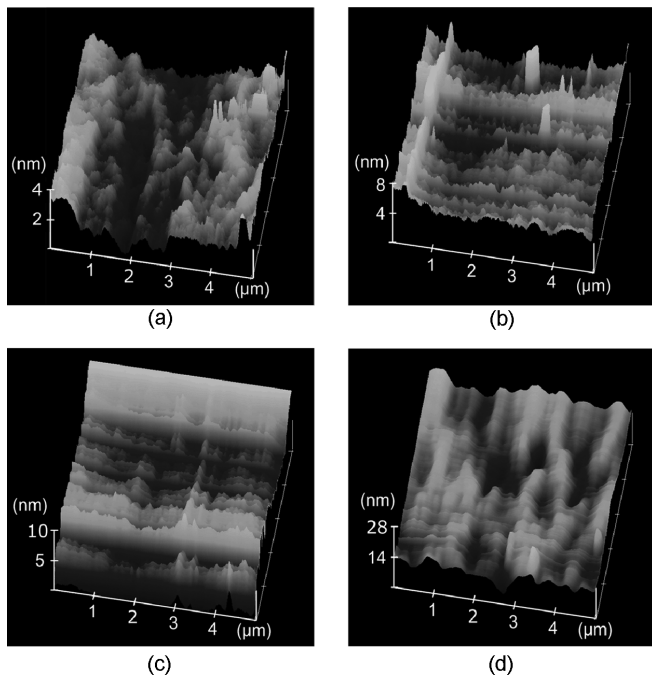


Fig. 5. Three-dimensional AFM images of BCB films illuminated by (a) 0 shot, (b) 30 shots, (c) 100 shots, and (d) 1000 shots.

To further investigate the UV-illuminated BCB surface, rms roughness values of BCB films are inspected by AFM. In order to improve the accuracy of the measurement, twelve samples are prepared. For each number of laser shots (i.e., 0, 30, 100, and 1000), three samples are measured. And the measurement is performed twice for each sample. The three-dimensional images scanned by contact-mode in an area of  $5 \times 5 \mu\text{m}^2$  are shown in Fig. 5. The rms roughness of the un-illuminated sample is 0.512 nm. For samples with 30 and 100 laser shots, the rms roughness values are 0.703 and 0.892 nm, respectively. The percentage of standard deviations are 4.32%, 5.36%, and 5.33% corresponding to the measured rms roughness values 0.512, 0.703, and 0.892 nm, respectively. Experimental results show that the rms roughness values of samples with below 100 laser shots are less than 0.9 nm, which are small enough for practical application. When 1000 laser shots are illuminated on the sample, the rms roughness abruptly increases to more than 2.300 nm with a deviation of 6.07%. This reveals the more the laser shots are illuminated, the more serious the surface damage is. According to the examination results of SEM and AFM, less than 100 laser shots are chosen to prevent material surface from being seriously damaged for all fabrications of optical waveguides.

The propagation loss is measured by transmission method [21]. This method avoids sample cutting and moving, so inevitable experimental inaccuracies can be reduced. In the measurement, planar waveguides and two sets of channel waveguides are both used. For each set, four samples with 30, 50, 70, and 100 laser shots are measured. For each sample, more than two waveguides are measured. The measured propagation loss of planar waveguide is 0.41 dB/cm with an error margin of  $\pm 0.15$  dB/cm, which represents the difference between the

TABLE V  
RELATION BETWEEN DEGREE OF CURE AND INDEX OF BCB FILM

| Curing condition | Index of film | Degree of cure(%) |
|------------------|---------------|-------------------|
| 210°C, 40 min    | 1.593         | 80.0              |
| 250°C, 1 h       | 1.571         | 96.0              |
| 280°C, 2 h       | 1.557         | 98.6              |

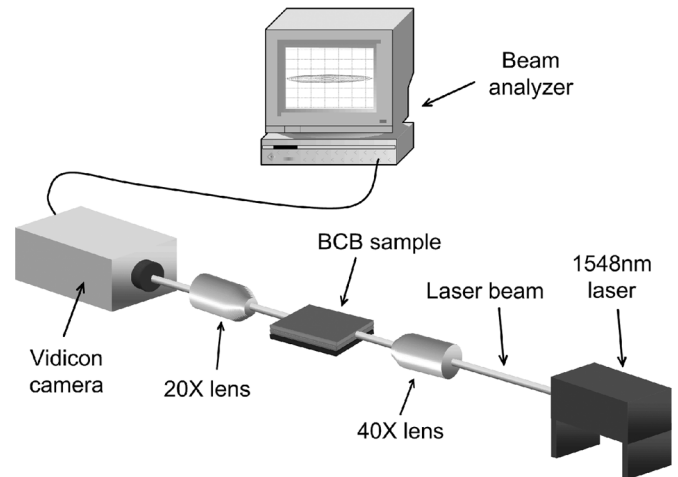


Fig. 6. Measurement setup for optical waveguides.

TABLE II  
CUT-OFF CONDITIONS OF THE BURIED-TYPE SINGLE-MODE CHANNEL WAVEGUIDES

| Mask width<br>( $\mu\text{m}$ ) | Number of laser shots |    |    |    |    |     |
|---------------------------------|-----------------------|----|----|----|----|-----|
|                                 | 10                    | 20 | 30 | 50 | 70 | 100 |
| 2                               | X                     | X  | X  | X  | X  | X   |
| 4                               | X                     | X  | X  | X  | O  | O   |
| 6                               | X                     | X  | O  | O  | O  | O   |
| 8                               | O                     | O  | O  | O  | O  | ⊙   |

X cut-off   O single-mode   ⊙ multimode

maximum and minimum loss. The measured propagation losses of channel waveguides at 1548 nm appear to be the same with different numbers of laser shots due to the small difference of damage caused by the laser shots. The average loss is estimated to be 0.6 dB/cm with an error margin of  $\pm 0.2$  dB/cm, which is just a little higher than that of planar waveguides.

The propagation loss is smaller than that of ridge-type BCB waveguides at wavelengths of 1300 [5] and 1548 nm [12], and even far smaller than that of ridge-type epoxy/BCB waveguides (2 dB/cm) [8]. That indicates the propagation losses of the proposed buried-type BCB channel waveguides are smaller.

### C. Adjustable Single-Mode Optical Waveguides

To find the cut-off conditions of single-mode channel waveguides at 1548 nm, a series of waveguides with different mask widths and laser shots are prepared. The measurement setup of optical fields is shown in Fig. 6. The results are listed in Table II. As can be seen, a waveguide of width 8  $\mu\text{m}$  supporting only single-mode can be fabricated with as few as 10 laser shots. However, for waveguides of narrower widths, such as 6 and 4

TABLE III  
POWER INTENSITY CONTOURS AND FWHMS OF SINGLE-MODE CHANNEL WAVEGUIDES WITH DIFFERENT WIDTHS

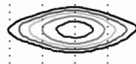


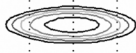

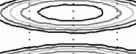
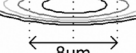
| Mask width ( $\mu\text{m}$ ) | Number of shots | Power intensity contours   | FWHM ( $\mu\text{m}$ ) | Simulated FWHM ( $\mu\text{m}$ ) | Error percentage |
|------------------------------|-----------------|--|------------------------|----------------------------------|------------------|
| 4                            | 70              |                     | 7.873                  | 7.632                            | 3.16%            |
| 6                            | 70              |                     | 8.135                  | 7.931                            | 2.57%            |
| 8                            | 70              | <br>6 $\mu\text{m}$ | 8.954                  | 8.672                            | 3.25%            |

TABLE IV  
POWER INTENSITY CONTOURS AND FWHMS OF SINGLE-MODE CHANNEL WAVEGUIDES INDUCED BY ILLUMINATING DIFFERENT NUMBERS OF LASER SHOTS

| Mask width ( $\mu\text{m}$ ) | Number of shots | Power intensity contours   | FWHM ( $\mu\text{m}$ ) | Simulated FWHM ( $\mu\text{m}$ ) | Error percentage |
|------------------------------|-----------------|--|------------------------|----------------------------------|------------------|
| 8                            | 70              |                     | 8.954                  | 8.672                            | 3.25%            |
| 8                            | 50              |                     | 9.227                  | 9.012                            | 2.39%            |
| 8                            | 30              |                     | 10.839                 | 10.523                           | 3.00%            |
| 8                            | 20              | <br>8 $\mu\text{m}$ | 11.625                 | 11.307                           | 2.81%            |

$\mu\text{m}$ , the minimum numbers of laser shots are increased to be 30 and 70, respectively. As for the waveguide of width  $2 \mu\text{m}$ , 200 laser shots are needed to support single-mode but the surface damage is too serious to be useful. Moreover, by the proposed UV-illumination method, different mode sizes can be easily obtained without further lithography and etching process. Based on the step-index profile, the simulated full-width at half-maximum (FWHM) of mode profiles are calculated for comparison. Table III shows measured modal power intensities, FWHMs, and simulated FWHMs of waveguides with different mask widths but illuminated with the same number of laser shots. We can see that the widths of optical power intensities are widened gradually from 4 to  $8 \mu\text{m}$ , yet with a uniform height of about  $1.7 \mu\text{m}$ . This shows the stability of the proposed method and that the UV pulses have been uniformly expanded for illumination. In addition, the measured FWHMs are close to the calculated ones. The maximum error is 3.25%, which shows good reproducibility of the fabrication method. Similarly, Table IV shows measured modal power intensities, FWHMs, and simulated FWHMs of waveguides with the same width of  $8 \mu\text{m}$  but fabricated with different numbers of laser shots. It can be seen that the optical confinement becomes better with increasing number of laser shots. Thus, waveguide mode sizes with different aspect ratios can be easily adjusted by the proposed UV-illumination method for higher coupling efficiency in optical interconnection [19].

Moreover, by the performance of directional couplers, the extent of lateral diffusion of  $\Delta n$  is estimated to be  $0.3 \mu\text{m}$ , which is small enough for practical application. The details of the performance of the directional coupler will be reported in the near future.

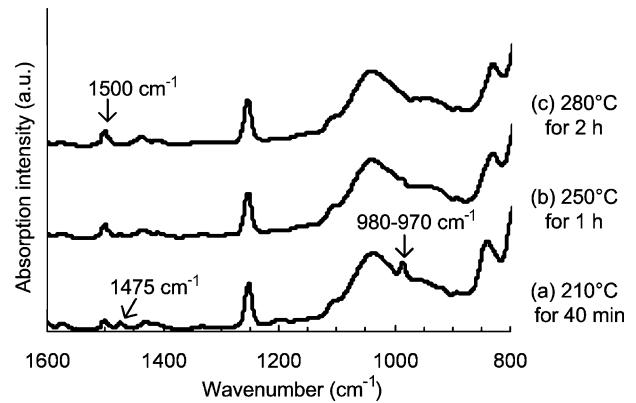


Fig. 7. IR absorption spectra under different curing conditions. (a)  $210 \text{ }^\circ\text{C}$  for 40 min. (b)  $250 \text{ }^\circ\text{C}$  for 1 h. (c)  $280 \text{ }^\circ\text{C}$  for 2 h.

#### D. Chemical Characterizations of BCB Film

In order to investigate the effect of the number of laser shots on index change, which related to the chemical mechanism behind the proposed UV-illumination, FTIR and XPS are examined to analyze the BCB films. In accordance to [20] and [22], the thermal curing process of BCB proceeds with a ring opening and then is followed by a Diels–Alder reaction. And the degree of cure in polymer is a function of temperature and time. Experimental results obtained under three different curing conditions ( $210 \text{ }^\circ\text{C}$  for 40 min,  $250 \text{ }^\circ\text{C}$  for 1 h, and  $280 \text{ }^\circ\text{C}$  for 2 h) are shown in Fig. 7 and Table V. It can be seen in Fig. 7, with an increasing of temperature and curing time, the peaks at  $1475$  and  $980\text{--}970 \text{ cm}^{-1}$  disappear but the peak at  $1500 \text{ cm}^{-1}$  becomes noticeable. The three

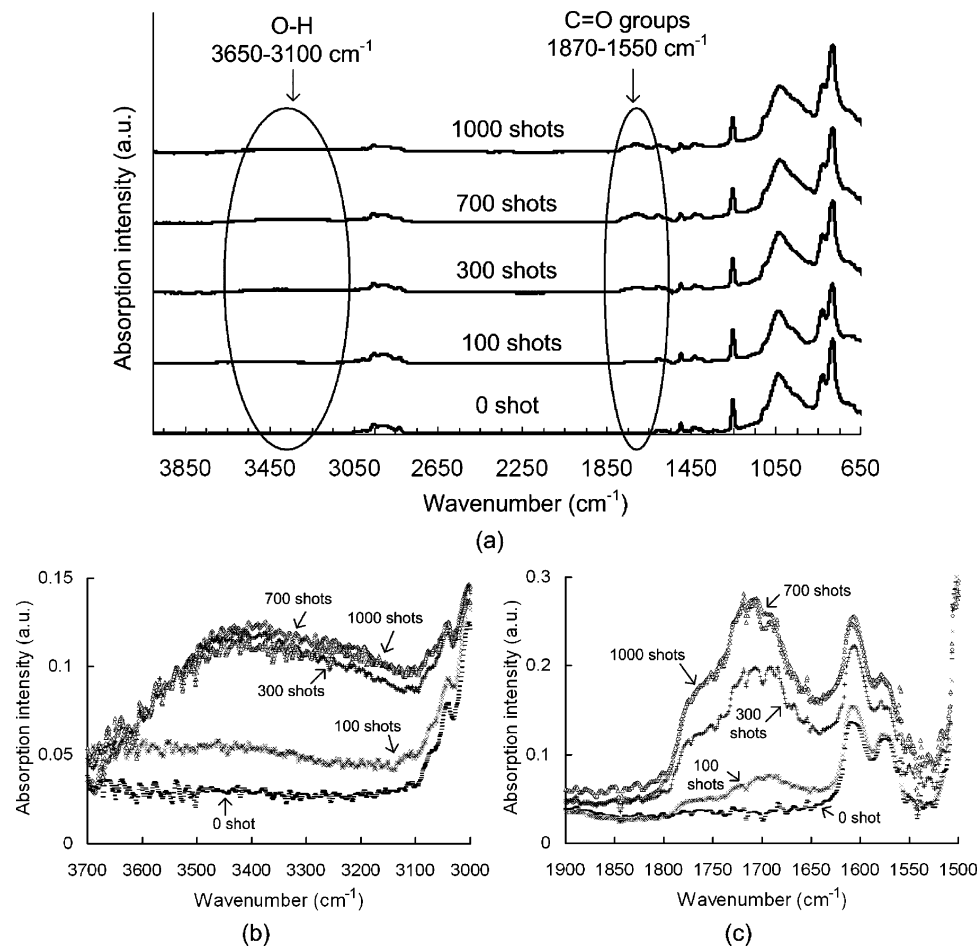


Fig. 8. IR absorption spectra of BCB films illuminated by different numbers of laser shots. (a) Whole spectra. (b) Local enlarged spectra for O–H bonds signal. (c) Local enlarged spectra for C=O bonds signal.

peaks represent the reacting BCB group, trimethylene oxide, and tetrahydronaphthalene, respectively [22]. The first two functional groups exist in BCB monomers and the last one exists in BCB polymers only. Due to the higher degree of the thermal curing process, more major functional groups of BCB monomer such as reacting BCB group and trimethylene oxide are reduced, and, on the contrary, the peak of tetrahydronaphthalene become more noticeable. Table V shows that indices of BCB films decrease with an increasing degree of cure, which is opposite to that found in UV-illumination. This indicates the proposed UV-illumination is not an additional curing process. After polymerization at 250 °C for 1 h, the infrared absorption spectrum of an un-illuminated BCB film measured by FTIR is shown in Fig. 8(a). The information of functional groups can be referenced in [23], such as C–H bond in benzene (3050–2840  $\text{cm}^{-1}$ ), Si–CH<sub>3</sub> bond (1253  $\text{cm}^{-1}$ ), Si–O–Si bond (1090–1020  $\text{cm}^{-1}$ ), and Si–(CH<sub>3</sub>)<sub>n</sub> groups ( $n = 2$  or 3) (860–760  $\text{cm}^{-1}$ ). A series of samples with different numbers of laser shots (i.e., 0, 10, 30, 50, 100, 200, 300, 500, 700, 800, and 1000) are measured by FTIR. In particular, the spectra of samples with 0, 100, 300, 700, and 1000 laser shots are shown in Fig. 8. We can see that the intensities of the two wavenumber regions become higher when the number of laser shots increases. The first region around 3300  $\text{cm}^{-1}$  (3650–3100  $\text{cm}^{-1}$ ) reveals the signals of various O–H bonds,

TABLE VI  
ATOM PERCENTAGES OF SAMPLES WITH DIFFERENT NUMBERS  
OF LASER SHOTS

| Number of laser shots | C (%) | O (%) | Si (%) |
|-----------------------|-------|-------|--------|
| 0                     | 86.48 | 3.25  | 10.27  |
| 30                    | 86.47 | 3.67  | 9.86   |
| 100                   | 83.70 | 6.40  | 9.90   |
| 1000                  | 82.80 | 7.62  | 9.58   |

and the second one (1870–1550  $\text{cm}^{-1}$ ) stands for various types of C=O bonds. Compared to the absorption spectrum of an un-illuminated BCB film, the two specific wavenumber regions can be enlarged as shown in Fig. 8(b) and (c). Clearly, the intensities of samples with less than 100 laser shots increase slightly, but grow faster with less than 300 laser shots. For 300 to 1000 laser shots, the increase of intensities becomes slower and tends to be saturated. The variation of the IR absorption spectrum intensity with the number of laser shots corresponds to the similar variation of the induced index changes as mentioned before. Moreover, un-illuminated BCB films and samples with 30, 100, and 1000 laser shots are measured by XPS. Major atoms such as C(1s), O(1s), and Si(2p) in BCB material are analyzed. The atomic percentages of samples with different laser shots are

listed in Table VI. As compared to the percentages of carbon and silicon atoms, the percentages of oxygen atom increase gradually from 3.25%, 3.67%, 6.40%, to 7.62% corresponding to 0, 30, 100, and 1000 laser shots, respectively, which also supports the results of added C=O bonds and H–O bonds in the FTIR measurement.

As the UV pulsed-laser is illuminated on the BCB film, oxygen atoms get into BCB material and link up with carbon and hydrogen atoms to form C=O and H–O bonds. With an increasing number of laser shots, the UV-assisted chemical reaction proceeds rapidly at the beginning and slows down gradually over 200 laser shots. When more than 300 laser shots are used, the reaction becomes saturated due to a less number of free carbon and hydrogen atoms in the BCB polymer. With this chemical mechanism, the index change dependent on the number of laser shots can be understood.

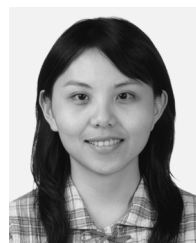
#### IV. CONCLUSION

In this paper, buried-type single-mode BCB optical waveguides fabricated by the UV pulsed-laser illumination method are proposed and comprehensively characterized. The fabrication method can not only simplify the fabrication process as requiring no further lithography and dry etching process, but also form buried-type channel waveguides to reduce propagation loss caused by sidewall roughness in conventional ridge-type channel waveguides. The measured propagation loss, 0.6 dB/cm at 1548 nm, is indeed lower than that of ridge-type BCB waveguides. The proposed method also provides a uniform step-like refractive index profile. Due to the flexibility, single-mode waveguides with different aspect ratios can be optimized for coupling into laser diodes to improve the coupling efficiency. Furthermore, the chemical mechanism behind the UV-illumination is carefully studied. Surface damage and rms roughness are inspected to locate the surface damage threshold of less than 100 laser shots. The chemical mechanism is further qualitatively analyzed to find that the appearances of O–H bonds and C=O bonds after UV-illumination induce the index change, and the changing tendency of functional groups is along with the saturation phenomenon of index change with respect to number of laser shots. In the meanwhile, oxygen atom percentage of BCB polymer is also found from 3.25% to 7.62% corresponding to 0 shot and 1000 shots by XPS, which supports the results of FTIR. As compared to conventional methods for the fabrication of BCB waveguides, the proposed UV pulsed-laser illumination method is simpler, more flexible, and more suitable for fabricating waveguides of lower propagation loss. Details of the application of the proposed method for the fabrication of BCB optical devices will be of great interest in the future.

#### REFERENCES

- [1] L. Robitaille, C. L. Callender, and J. P. Noad, "Design and fabrication of low-loss polymer waveguide components for onchip optical interconnection," *IEEE Photon. Technol. Lett.*, vol. 8, no. 12, pp. 1647–1649, Dec. 1996.
- [2] M. C. Oh, H. Zhang, C. Zhang, H. Erlig, Y. Chang, B. Tsap, D. Chang, A. Szep, W. H. Steier, H. R. Fetterman, and L. R. Dalton, "Recent advances in electro-optic polymer modulators incorporating highly nonlinear chromophore," *IEEE J. Sel. Topics Quantum Electron.*, vol. 7, no. 5, pp. 826–835, Sep. 2001.

- [3] K. K. Tung, W. H. Wong, and E. Y. B. Pun, "Polymeric optical waveguides using direct ultraviolet photolithography process," *Appl. Phys. A: Mater. Sci. Process.*, vol. 80, no. 3, pp. 621–626, Feb. 2005.
- [4] S. W. Seo, S. Y. Cho, and N. M. Jokerst, "A thin-film laser, polymer waveguide, and thin-film photodetector cointegrated onto a silicon substrate," *IEEE Photon. Technol. Lett.*, vol. 17, no. 10, pp. 2197–2199, Oct. 2005.
- [5] C. F. Kane and R. R. Krchnavek, "Benzocyclobutene optical waveguides," *IEEE Photon. Technol. Lett.*, vol. 7, no. 5, pp. 535–537, May 1995.
- [6] S. Y. Cho, M. K. Brooke, and N. M. Jokerst, "Optical interconnections on electrical boards using embedded active optoelectronic components," *IEEE J. Sel. Topics Quantum Electron.*, vol. 9, no. 3, pp. 465–476, Mar. 2003.
- [7] L. L. W. Leung, W. C. Hon, and K. J. Chen, "Low-loss coplanar waveguides interconnects on low-resistivity silicon substrate," *IEEE Trans. Compon., Packag., Manuf. Technol.*, vol. 27, no. 3, pp. 507–512, Sep. 2004.
- [8] K. P. Lor, Q. Liu, and K. S. Chiang, "UV-written long-period gratings on polymer waveguides," *IEEE Photon. Technol. Lett.*, vol. 17, no. 3, pp. 594–596, Mar. 2005.
- [9] P. E. Garrou, R. H. Heistand, M. G. Dibbs, T. A. Mainal, T. M. Stokich, P. H. Townsend, G. M. Adema, M. J. Berry, and I. Turlik, "Rapid thermal curing of BCB dielectric," *IEEE Trans. Comp., Packag., Technol.*, vol. 16, no. 1, pp. 46–52, Feb. 1993.
- [10] A. Straat and F. Nikolajeff, "Study of benzocyclobutene as an optical material at elevated temperatures," *Appl. Opt.*, vol. 40, no. 29, pp. 5147–5152, Oct. 2001.
- [11] S. Y. Cheng, K. S. Chiang, and H. P. Chan, "Birefringence in benzocyclobutene strip optical waveguides," *IEEE Photon. Technol. Lett.*, vol. 15, no. 5, pp. 700–703, May 2003.
- [12] C. W. Hsu, H. L. Chen, W. C. Chao, and W. S. Wang, "Characterization of benzocyclobutene optical waveguides fabricated by electron-beam direct writing," *Microw. Opt. Technol. Lett.*, vol. 42, no. 2, pp. 208–210, Aug. 2004.
- [13] Q. Liu, K. S. Chiang, and K. P. Lor, "Long-period gratings in polymer ridge waveguides," *Opt. Exp.*, vol. 13, no. 4, pp. 1150–1160, Feb. 2005.
- [14] Y. G. Zhao, W. K. Lu, Y. Ma, S. S. Kim, and S. T. Ho, "Polymer waveguides useful over a very wide wavelength range from the ultraviolet to infrared," *Appl. Phys. Lett.*, vol. 77, no. 19, pp. 2961–2963, Nov. 2000.
- [15] D. G. Rabus, P. Henzi, and J. Mohr, "Photonic integrated circuits by DUV-induced modification of polymers," *IEEE Photon. Technol. Lett.*, vol. 17, no. 3, pp. 591–593, Mar. 2005.
- [16] L. Y. Chen, W. S. Tsai, W. H. Hsu, K. Y. Chen, T. J. Wang, and W. S. Wang, "Characterization of UV-Induced benzocyclobutene optical waveguides," presented at the IEEE Conf. Lasers Electro-Optics (CLEO), Long Beach, CA, May 2006, Paper JWB53.
- [17] C. F. Kane and R. R. Krchnavek, "Processing and characterization of benzocyclobutene optical waveguides," *IEEE Trans. Compon. Packag. Manuf. Technol. B*, vol. 18, no. 3, pp. 565–571, Aug. 1995.
- [18] J. M. White and P. F. Heidrich, "Optical waveguide refractive index profiles determined from measurement of mode indices: a simple analysis," *Appl. Opt.*, vol. 15, no. 1, pp. 151–155, Jan. 1976.
- [19] B. B. Goldberg, M. S. Unlu, W. D. Herzog, H. F. Ghaemi, and E. Towe, "Near-field optical studies of semiconductor heterostructures and laser diodes," *IEEE J. Sel. Topics Quantum Electron.*, vol. 1, no. 6, pp. 1073–1081, Dec. 1995.
- [20] Dow Chemical Company. Midland, MI.
- [21] W. J. Wang, S. Honkanen, S. I. Najafi, and A. Tervonen, "Loss characteristics of potassium and silver double-ion-exchanged glass waveguides," *J. Appl. Phys.*, vol. 74, pp. 1529–1533, Apr. 1993.
- [22] R. V. Taniikella, S. A. B. Allen, and P. A. Kohl, "Variable-frequency microwave curing of benzocyclobutene," *J. Appl. Polym. Sci.*, vol. 83, pp. 3055–3067, Apr. 2002.
- [23] G. Socrates, *Infrared Characteristic Group Frequencies*. New York: Wiley, 1980.



**Liang-Yin Chen** (S'05) was born in Taipei, Taiwan, R.O.C., in December 1979. She received the B.S. degree in chemical engineering from National Taiwan University (NTU), Taipei, Taiwan, R.O.C., in 2002, where she is currently working toward the Ph.D. degree.

She joined the Integrated Optics Laboratory, NTU, in 2002. Her research interests include the design and fabrication of optical devices such as polymer optical waveguides, ridge waveguides, and surface plasmon resonance optical sensors.



**Wan-Shao Tsai** (S'04) was born on February 7, 1980, in Taichung, Taiwan, R.O.C. She received the B.S. degree in electrical engineering from National Taiwan University, Taipei, Taiwan, R.O.C., in 2002, where she is currently working toward the Ph.D. degree in the Graduate Institute of Electronics Engineering.

Her research interests include the design and fabrication of integrated optical waveguides, near-field measurement, and numerical simulation.



**Kuan-Yu Chen** was born in Taipei, Taiwan, R.O.C., in May 1982. He received the B.S. degree in electrical engineering and the M.S. degree in electro-optical engineering from National Taiwan University, Taipei, Taiwan, R.O.C., in 2004 and 2006, respectively.

His current research is focused on the design and fabrication of polymer optical waveguides.



**Wen-Hao Hsu** was born in Taipei, Taiwan, R.O.C., in 1976. He received the B.S. degree in electrical engineering, and the M.S. and Ph.D. degrees in electro-optical engineering from National Taiwan University (NTU), Taipei, Taiwan, R.O.C., in 1999, 2001, and 2006, respectively.

He joined the Integrated Optics Laboratory, NTU, since 1998. His research interests included electro-optic waveguide devices, optical waveguide sensors, and short-wavelength dielectric waveguides.



**Way-Seen Wang** (M'84) was born in 1948, in Taipei, Taiwan, R.O.C. He received the B.S. degree in electrical engineering from National Taiwan University (NTU), Taipei, Taiwan, R.O.C., in 1970, and the M.S. and Ph.D. degrees from University of Southern California, Los Angeles, in 1975 and 1979, respectively.

Since August 1971, he has been with the Department of Electrical Engineering, NTU. In 1984, he became a Full Professor. His current research interest includes the design and fabrication of integrated optical waveguide devices.